Earthquakes and Structures, *Vol. 17, No. 3 (2019) 257-270*
DOI: https://doi.org/10.12989/eas.2019.17.3.257

Bending behavior of laminated composite plates using the refined four-variable theory and the finite element method

Mokhtar Bouazza*[1,3], Tawfiq Becheri[1], Abderrahmane Boucheta[1] and Noureddine Benseddiq[2]

[1]Department of Civil Engineering, University Tahri Mohamed of Bechar, Bechar 08000, Algeria
[2]Mechanics Laboratory of Lille, CNRS UMR 8107, University of Lille 1, 59655 Villeneuve d'Ascq, France
[3]Laboratory of Materials and Hydrology (LMH), University of Sidi Bel Abbes, Sidi Bel Abbes 2200, Algeria

(*Received September 29, 2019, Revised May 12, 2019, Accepted June 10, 2019*)

Abstract. The purpose of this work is to analyze the bending behavior of laminated composite plates using the refined four-variable theory and the finite element method approach using an ANSYS 12 computational code. The analytical model is based on the multilayer plate theory of shear deformation of the nth-order proposed by Xiang *et al* 2011 using the theory principle developed by Shimpi and Patel 2006. Unlike other theories, the number of unknown functions in the present theory is only four, while five or more in the case of other theories of shear deformation. The formulation of the present theory is based on the principle of virtual works, it has a strong similarity with the classical theory of plates in many aspects, it does not require shear correction factor and gives a parabolic description of the shear stress across the thickness while filling the condition of zero shear stress on the free edges. The analysis is validated by comparing results with those in the literature.

Keywords: laminated; bending; refined nth-order shear deformation theory; finite element method

1. Introduction

In recent years, laminated composite plate analysis has undergone a considerable evolution and a variety of plate theories have been introduced as a function of the transverse deformation effect of the shear. Classical plate theory (CPT), which neglects the deformation effect of transverse shear, provides reasonable results for thin plates. Reissner (1945) and Mindlin (1951) developed the first-order theory that takes into account the effects of transverse shear across thickness (FSDT). This theory requires shear correction factors to correct the variation of transverse shear stresses and shear deformations across the thickness. These shear correction factors are sensitive not only to the geometrical parameters of the plate, but also to the boundary conditions and loading conditions.

To avoid the use of shear correction factors, some authors have adopted higher order theories HSDT. Various shear deformation plate (HSDT) theories have been proposed, Whitney and Sun (1973) which assumed a displacement field of order greater than 3. This theory is complicated and has given precise results. Other theories appeared later, each of them presents advantages and disadvantages with different formalisms according to the field of application. For example, Lo *et al*. (1977) proposed a theory with eleven unknowns; Bhimaraddi and Stevens (1984) with five unknowns; Reddy (1984), Reddy and Phan (1985), five unknowns and Hanna and Leissa (1994) to four unknowns. Ambartsumian (1969) proposed a transverse stress function to explain plate deformation. A similar method was used by Soldatos and Timarci (1993) for the dynamic analysis of laminated hulls. Later, new functions were proposed by Reddy (1984), Senthilnathan *et al*. (1987), Touratier (1991), Soldatos (1992), Karama *et al.* (2003), Aydogdu (2009), Xiang *et al.* (2011a) and Mantari *et al.* (2012).

El-Abbasi and Meguid (2000) devlopped new shell element accounting for through thickness deformation. To analyze the bending and transverse shear effects of laminated composite plates, a new higher-order thirteen nodes triangular element presented by Rezaiee-Pajand *et al.* (2012). Patel (2014) studied the bending analysis of laminated composite stiffened plates subjected to uniform transverse loading with the geometric nonlinear. Structural performance of ribbed ferrocement plates reinforced with composite materials presented by Yousry *et al.* (2016). Two triangular shell element having three and six nodes are presented by Rezaiee-Pajand *et al.* (2018) analysis the for geometrically nonlinear of thin and thick shell structures. Kim and Bathe (2008) presented three-dimensional shell element to model shell surface tractions and incompressible behavior. The geometrically nonlinear formulation for a six-node triangular shell element is proposed by Rezaiee-Pajand *et al.* (2018). Chen (2016) studied the Effect of local wall thinning on ratcheting behavior of pressurized 90° elbow pipe under reversed bending using finite element analysis. Isoparametric six-node triangular element is utilized by Rezaiee-Pajand (2018) for geometrically nonlinear analysis of functionally graded (FG) shells.

The effects of moisture and temperature on buckling of laminated composite cylindrical shell panels are investigated numerically and experimentally by Biswal *et al.* (2016). Based on the continuum mechanic's theory, a 6-

*Corresponding author, Professor
E-mail: bouazza_mokhtar@yahoo.fr

ISSN: 2092-7614 (Print), 2092-7622 (Online)

node triangular isoparametric element is formulated by Rezaiee-Pajand and Arabi (2016) for analysis geometrically nonlinear of laminated shells. Large deformation bending analysis and nonlinear flexural vibration of functionally graded spherical shell using FEM studied by Kar and Panda (2015).

On the other hand, a theory of Variable Refined Plate (RPT) was first developed for isotropic plates by Shimpi (2002) and extended to orthotropic plates by Shimpi and Patel (2006), Kim *et al*. (2009) and Thai and Kim (2010) used this theory to study laminated composite plates. Piscopo (2010) studied the buckling of rectangular plates under uni-axial and bi-axial compression by refined theory. Narendar (2011) studied the mechanical buckling of nanoplates and Thai (2012) developed a refined, non-local theory of nanobeams. Thai and Choi (2012) developed the efficient and simple refined theory for the buckling analysis of functionally graded plates. Adim *et al.* (2018) used simple higher order shear theory to analyze mechanical buckling analysis of hybrid laminated composite plates under different boundary conditions. Hebali *et al*. (2014) proposed a novel four variable refined plate theory for static bending, buckling, and vibration of functionally graded plates. Ait Amar Meziane *et al.* (2014) studied the buckling and free vibration response of functionally graded exponential sandwich plates (FGM) under various boundary conditions. Becheri *et al.* (2016) studied analytical buckling of symmetrically laminated plates using nth-order shear deformation theory with curvature effects. Hamidi *et al*. (2015) investigated the thermomechanical bending of functional gradient sandwich plates using a sinusoidal plate theory with 5 unknowns taking into account the stretching effect. Bouazza *et al*. (2016) developed an analytical solution of refined theory of hyperbolic shear deformation to obtain the critical buckling temperature of simply supported cross-laminated plates. Reza Barati and Shahverdi (2016) studied thermal vibration of embedded FG nanoplates under non-uniform temperature distributions with different boundary conditions using four-variable plate theory. Analytical solution for mechanical buckling analysis of magnetoelectroelastic plate resting on pasternak foundation based on the third-order shear deformation plate theory investigated by Ellali *et al.* (2018). Hygrothermal effects on the free vibration behavior of composite plate using nth-order shear deformation theory and micromechanical approach presented by Abdelmalek *et al.* (2019). A nonlocal trigonometric shear deformation plate theory was introduced for thermal buckling analysis of functionally graded embedded nanosize plates by Khetir *et al.* (2017). Younsi *et al.* (2018) have suggested a 3D and 2D refined shear deformation theory taking under consideration transverse shear deformation effects presented for the bending and free vibration analysis of FG plates. Bouhadra *et al.* (2018) have studied advanced composite plates using higher shear deformation theory (HSDT) to consider the influence of thickness stretching in functionally graded plates. Moreover, survey of literature indicates that the thermal buckling of FG plates has been widely investigated. Some researches were presented on the linear thermal buckling and vibration analysis of advance plates (Bousahla *et al.* 2016, Bouazza *et al.* 2017, 2018, Menasria *et al.* 2017, Chikh *et al.* 217, Bourada *et al.* 2019, Fourn *et al.* 2017, Antar *et al.* 2019).

This section deals with the theory of nth-order shear deformation (Xiang *et al*. 2011a). The effectiveness and precision of this theory is demonstrated by (Xiang *et al*. 2011b, 2012, 2013a, b). Moreover, in this part we use mainly the ideas of the new theory of refined plates established by Shimpi (2002) that the author includes w_b and w_s to model the transverse displacement (transverse displacement of bending and shear) instead of the constant displacement assumption w_0 (Mantari *et al.* 2012, Xiang *et al.* 2011a, 2012, 2013a, b). To the best of the authors' knowledge, there are no studies in the open literature on bending behaviors of laminated composite plate via nth-order four shear deformation theory. With the increased usage of these materials, it is important to understand the behaviors of composite structures subjected to different mechanical loads. In this paper, these ideas are combined to develop a new theory of nth-order deformation with displacement field modification. Unlike other theories, this theory requires only four unknown functions, compared to five in the other shear deformation theories. The presented theory is strongly similar to classical plate theory in many aspects. It does not require the shear correction factor and causes the transverse shear stress variation so that the transverse shear stresses vary parabolically throughout the thickness to satisfy the conditions of the upper and lower shear stress free surfaces. The solution of the mechanical buckling analysis of symmetric multilayer laminated sheets is obtained. Numerical examples are presented to verify the accuracy of this theory.

2. Laminated plate modeling

2.1 Numerical modeling by ANSYS software

The software chosen is the ANSYS version 12 Nakasone (2006), marketed by ANSYS, Inc. It is one of the most used and best known software in the world for its various functionalities. With a wide choice of element types, material models, this software can cover a wide range of current engineering problems.

2.1.1 Choice of the type of element

In this work we chose the element Shell99 to model the laminated plates. Shell99 is a shell element that is suitable for modeling laminated composite structures (250 layers). The element is defined by eight nodes, each node has six degrees of freedom, three nodal translations following (x,y,z) and three rotations around the axes (x,y,z). A triangular-shaped element may be formed by defining the same node number for nodes K, L and O. The geometry, node locations, and the coordinate system for this element are shown in Fig. 1.

2.1.2 Mesh plates

For reasons of symmetry, we modeled only 1/4 of the plate. As for the density of the mesh, the finer the mesh, the

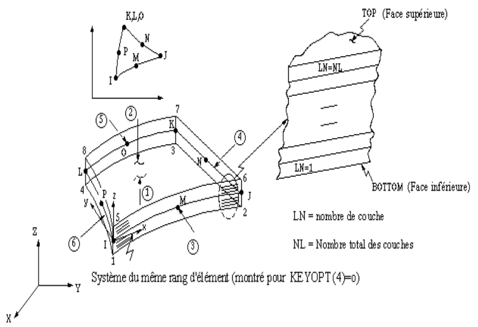

Fig. 1 Shell99 geometry (Nakasone 2006)

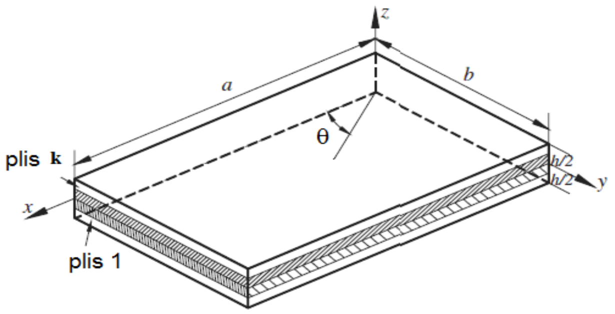

Fig.3 Form of laminated composite plate (Reddy 1997)

more the accuracy improves but the calculation time increases accordingly. A uniform mesh of 25 × 25 is made to mesh the isotropic plates and multilayer plates. Figure 2b shows an example of plate meshing which contains 625 elements and 1976 nodes. The figure2a show ¼ of the plate modeling by finite element method and boundary conditions.

2.2 Analytical modeling

2.2.1 Mathematical formulation

2.2.1.1 Kinematic

We consider a rectangular plate of length, a, width, b, thickness, h, and fibre angle θ defined in its system of axes (x, y, z), see Fig. 3. In which θ is the angle between the global x-axis and the local x-axis of each lamina. The laminated plate consists of k layers of equal thickness. In this part, additional simplifying assumptions are made to the n-shear deformation theory so that the number of unknowns is reduced. The displacement field of the n-shear deformation theory is given by Xiang *et al* (2011a).

$$\begin{aligned}
u_1(x,y,z) &= u(x,y) + z\phi_x(x,y) - \frac{1}{n}\left(\frac{2}{h}\right)^{n-1} z^n \left(\phi_x(x,y) + \frac{\partial w(x,y)}{\partial x}\right)\\
u_2(x,y,z) &= v(x,y) + z\phi_y(x,y) - \frac{1}{n}\left(\frac{2}{h}\right)^{n-1} z^n \left(\phi_y(x,y) + \frac{\partial w(x,y)}{\partial y}\right)\\
n &= 3,5,7,9,........\\
u_3(x,y,z) &= w_0(x,y)
\end{aligned} \tag{1}$$

Where u_1, u_2, u_3 are displacements in the x, y, z directions, w_0, ϕ_x and ϕ_y: are unknown displacement functions of the mean plane of the plate.

By dividing the transverse displacement $w_0$into bending and shearing parts ($w_0=w_b+w_s$) and making other hypotheses given by $\phi_x=-\partial w_b/\partial x$ and $\phi_y=-\partial w_b/\partial y$, Substituting ($w_0=w_b+w_s$, $\phi_x=-\partial w_b/\partial x$) and $\phi_y=-\partial w_b/\partial y$ into Eq. (1), the following equation is obtained

$$\begin{aligned}
u_1(x,y,z) &= u(x,y) - z\frac{\partial w_b}{\partial x} - \frac{1}{n}\left(\frac{2}{h}\right)^{n-1} z^n \left(\left(-\frac{\partial w_b}{\partial x}\right) + \frac{\partial(w_b+w_s)}{\partial x}\right)\\
u_2(x,y,z) &= v(x,y) - z\frac{\partial w_b}{\partial y} - \frac{1}{n}\left(\frac{2}{h}\right)^{n-1} z^n \left(\left(-\frac{\partial w_b}{\partial y}\right) + \frac{\partial(w_b+w_s)}{\partial y}\right)\\
n &= 3,5,7,9,........\\
u_3(x,y,z) &= w_b(x,y) + w_s(x,y)
\end{aligned} \tag{2}$$

By simplifying the displacement field of the new refined theory can be written in a simpler form as follow

$$\begin{aligned}
u_1(x,y,z) &= u(x,y) - z\frac{\partial w_b}{\partial x} - \frac{1}{n}\left(\frac{2}{h}\right)^{n-1} z^n \left(\frac{\partial w_s}{\partial x}\right)\\
u_2(x,y,z) &= v(x,y) - z\frac{\partial w_b}{\partial y} - \frac{1}{n}\left(\frac{2}{h}\right)^{n-1} z^n \left(\frac{\partial w_s}{\partial y}\right)\\
n &= 3,5,7,9,........\\
u_3(x,y,z) &= w_b(x,y) + w_s(x,y)
\end{aligned} \tag{3}$$

The displacement field of the present theory is chosen on the basis of the following assumptions:

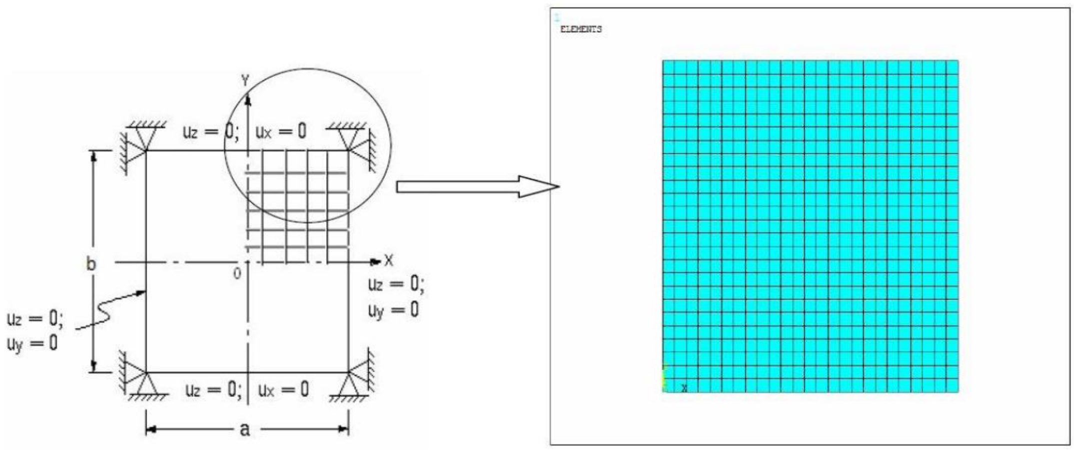

Fig. 2 Plate modeling by finite element method and boundary conditions

(1) The parts of the bending components $-z\partial w_b/\partial x$ and $-z\partial w_b/\partial y$ in the plane are similar to those given by the classical laminated plate theory (CLPT).

(2) The parts of shear components $-\frac{1}{n}\left(\frac{2}{h}\right)^{n-1} z^n\left(\frac{\partial w_s}{\partial x}\right)$ and $-\frac{1}{n}\left(\frac{2}{h}\right)^{n-1} z^n\left(\frac{\partial w_s}{\partial y}\right)$ in the plane give rise to parabolic variations of shear deformations and thus to shear stresses across the thickness of the plate so that zero shear stresses on the upper and lower faces.

2.2.1.2 Stress-strain relationship

The stresses in the main axes of the layer k can also be obtained from the deformations expressed in the main axes. The stresses are expressed as follows

$$\begin{Bmatrix}\sigma_x\\ \sigma_y\\ \sigma_{xy}\end{Bmatrix}=\begin{bmatrix}Q_{11} & Q_{12} & 0\\ Q_{12} & Q_{22} & 0\\ 0 & 0 & Q_{66}\end{bmatrix}\begin{Bmatrix}\varepsilon_x\\ \varepsilon_y\\ \gamma_{xy}\end{Bmatrix} \tag{4a}$$

$$\begin{Bmatrix}\sigma_{yz}\\ \sigma_{xz}\end{Bmatrix}=\begin{bmatrix}Q_{44} & 0\\ 0 & Q_{55}\end{bmatrix}\begin{Bmatrix}\gamma_{yz}\\ \gamma_{xz}\end{Bmatrix} \tag{4a}$$

Where

σ_x, σ_y and σ_{xy}: In-plane stresses, σ_{yz} and σ_{xz} shear stresses

γ_{xz}, γ_{yz}: The transverse shear strains

Q_{ij}: the reduced elastic constants of the material in the axes of the plate. These constants according to the modulus of elasticity in the principal axes give by

$$Q_{11}=\frac{E_1}{1-\nu_{12}\nu_{21}},\; Q_{12}=\frac{\nu_{12}E_2}{1-\nu_{12}\nu_{21}},\; Q_{22}=\frac{E_2}{1-\nu_{12}\nu_{21}},\quad Q_{66}=G_{12},\; Q_{44}=G_{23},\; Q_{55}=G_{13} \tag{5}$$

Where

E_1 and E_2 are Young's moduli along and transverse to the fibre, respectively

G_{12}, G_{23} and G_{13} In-plane and transverse shear moduli

ν_{12} and ν_{21} Poisson's ratios along and transverse to the fibre, respectively.

The stresses in layer k are expressed according to the general relation as follows

$$\begin{Bmatrix}\sigma_x\\ \sigma_y\\ \sigma_{xy}\end{Bmatrix}^{(k)}=\begin{bmatrix}\overline{Q}_{11} & \overline{Q}_{12} & \overline{Q}_{16}\\ \overline{Q}_{12} & \overline{Q}_{26} & \overline{Q}_{26}\\ \overline{Q}_{16} & \overline{Q}_{26} & \overline{Q}_{66}\end{bmatrix}^{(k)}\begin{Bmatrix}\varepsilon_x\\ \varepsilon_y\\ \gamma_{xy}\end{Bmatrix}^{(k)} \tag{6a}$$

$$\begin{Bmatrix}\sigma_{yz}\\ \sigma_{xz}\end{Bmatrix}^{(k)}=\begin{bmatrix}\overline{Q}_{44} & \overline{Q}_{45}\\ \overline{Q}_{45} & \overline{Q}_{55}\end{bmatrix}^{(k)}\begin{Bmatrix}\gamma_{yz}\\ \gamma_{xz}\end{Bmatrix}^{(k)} \tag{6b}$$

Where

k Number of layers

The parameters $\overline{Q}_{ij}$ of layer k are related to the reference axes of the laminate as shown in Fig. 4. They are expressed according to the parameters expressed in the axes of the materials of the layers. Their expressions are given by the expressions below

$$\overline{Q}_{ij}=T_1^{-1}Q_{ij}T_1 \quad (i,j=1,2,6)$$
$$\overline{Q}_{lm}=T_2^{-1}Q_{lm}T_2 \quad (l,m=4,5) \tag{7}$$

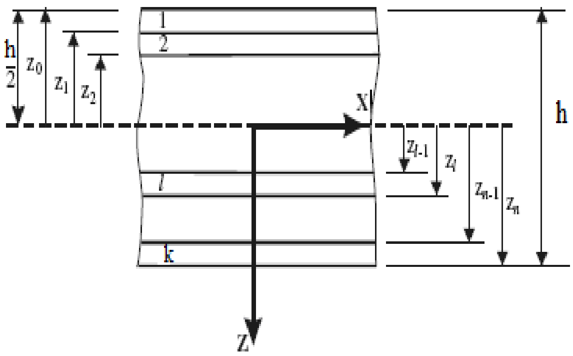

Fig. 4 Cross section of an n-layered laminate

With

Where T_1 and T_2 are the transformation matrix. The superscript (–1) denotes the matrix inverse.

$$T_1=\begin{bmatrix}\cos^2\theta & \sin^2\theta & 2\sin\theta\cos\theta\\ \sin^2\theta & \cos^2\theta & -2\sin\theta\cos\theta\\ -\sin\theta\cos\theta & \sin\theta\cos\theta & \cos^2\theta-\sin^2\theta\end{bmatrix} \tag{8a}$$

$$T_2=\begin{bmatrix}\cos\theta & -\sin\theta\\ \sin\theta & \cos\theta\end{bmatrix} \tag{8b}$$

2.2.1.3 The strain-displacements relations

The deformation components associated with the displacements in Eq. (l) are

$$\{\varepsilon\}=\{\varepsilon^0\}+\{k^b\}z+\{k^s\}f(z)$$
$$\begin{Bmatrix}\gamma_{yz}\\ \gamma_{xz}\end{Bmatrix}=\begin{Bmatrix}\gamma_{yz}^s\\ \gamma_{xz}^s\end{Bmatrix}g(z) \tag{9}$$

With

$$\{\varepsilon\}=\{\varepsilon_x,\varepsilon_y,\gamma_{xy}\}^T,\; \{\varepsilon^0\}=\{\varepsilon_x^0,\varepsilon_y^0,\gamma_{xy}^0\}^T=\left\{\frac{\partial u}{\partial x},\frac{\partial v}{\partial y},\frac{\partial u}{\partial y}+\frac{\partial v}{\partial x}\right\}^T$$

$$\{k^b\}=\{k_x^b,k_y^b,k_{xy}^b\}^T=\left\{-\frac{\partial^2 w_b}{\partial x^2},-\frac{\partial^2 w_b}{\partial y^2},-2\frac{\partial^2 w_b}{\partial x\partial y}\right\}^T$$

$$\{k^s\}=\{k_x^s,k_y^s,k_{xy}^s\}^T=\left\{-\frac{\partial^2 w_s}{\partial x^2},-\frac{\partial^2 w_s}{\partial y^2},-2\frac{\partial^2 w_s}{\partial x\partial y}\right\}^T \tag{10}$$

$$\gamma_{xz}^s=\frac{\partial w_s}{\partial x},\quad \gamma_{yz}^s=\frac{\partial w_s}{\partial y},\quad f(z)=\frac{1}{n}\left(\frac{2}{h}\right)^{n-1}z^n,$$

$$g(z)=1-\left(\frac{2z}{h}\right)^{n-1}$$

2.2.1.4 Kinematics constitutive equation and equilibrium equations

The energy of deformation of the plate can be written as follows

$$U=\frac{1}{2}\int_V \sigma_{ij}\varepsilon_{ij}dV$$
$$=\frac{1}{2}\int_V\left(\sigma_x\varepsilon_x+\sigma_y\varepsilon_y+\sigma_{xy}\gamma_{xy}+\sigma_{yz}\gamma_{yz}+\sigma_{xz}\gamma_{xz}\right)dV \tag{11}$$

By replacing the Eqs. (6a), (6b) and (9) in equation (11) and integrating across the plate thickness, the strain energy of the plate is written as follows

$$U=\frac{1}{2}\int_A\left[N_x\delta\varepsilon_x^0+N_y\delta\varepsilon_y^0+N_{xy}\delta\gamma_{xy}^0+M_x^b\delta k_x^b+M_y^b\delta k_y^b+\right.\\ \left.M_{xy}^b k_{xy}^b+M_x^s k_x^s+M_y^s k_y^s+M_{xy}^s k_{xy}^s+Q_{yz}^s\gamma_{yz}^s+Q_{xz}^s\gamma_{xz}^s\right]dxdy \tag{12}$$

The resulting forces and moments acting on a laminate can be obtained by integrating the stresses through the thickness of the plates, as shown below

$$\{N\}=\int_{-h/2}^{h/2}\sigma\ dz=\sum_{k=1}^{N}\int_{Z_k}^{Z_{k+1}}\sigma\ dz\\ =[A]\{\varepsilon^0\}+[B]\{k^b\}+[B^s]\{k^s\} \tag{13a}$$

$$\{M^b\}=\int_{-h/2}^{h/2}\sigma\ zdz=\sum_{k=1}^{N}\int_{Z_k}^{Z_{k+1}}\sigma\ zdz\\ =[B]\{\varepsilon^0\}+[D]\{k^b\}+[D^s]\{k^s\} \tag{13b}$$

$$\{M^s\}=\int_{-h/2}^{h/2}\sigma\ f(z)dz=\sum_{k=1}^{N}\int_{Z_k}^{Z_{k+1}}\sigma\ f(z)dz\\ =[B^s]\{\varepsilon^0\}+[D^s]\{k^b\}+[H^s]\{k^s\} \tag{13c}$$

With

$$\{N\}=\{N_x,N_y,N_{xy}\}^T\\ \{M^b\}=\{M_x^b,M_y^b,M_{xy}^b\}^T\\ \{M^s\}=\{M_x^s,M_y^s,M_{xy}^s\}^T \tag{14}$$

In the above expressions, the coefficients A_{ij} and B_{ij} in matrices [A], [B], etc. indicate the rigidity of the plate, which can be defined as

$$(A_{ij},B_{ij},D_{ij})=\int_{-h/2}^{h/2}\overline{Q}_{ij}(1,z,z^2)dz\\ (B_{ij}^s,D_{ij}^s,H_{ij}^s)=\int_{-h/2}^{h/2}\overline{Q}_{ij}(f(z),zf(z),(f(z))^2)dz\\ (i,j=1,2,6) \tag{15}$$

In Eq. (14), A_{ij} is the extensional stiffness matrix because it is associated with the plate in-plane behaviour. D_{ij} is the bending stiffness matrix and B_{ij} refers to the coupling between the laminate bending and extension.

The transverse shear force that can be defined as follows

$$\begin{Bmatrix}Q_{yz}\\ Q_{xz}\end{Bmatrix}=\begin{bmatrix}A_{44}^s & A_{45}^s\\ A_{54}^s & A_{55}^s\end{bmatrix}\begin{Bmatrix}\gamma_{yz}^s\\ \gamma_{xz}^s\end{Bmatrix} \tag{16}$$

With

$$A_{ij}^s=\int_{-h/2}^{h/2}\overline{Q}_{ij}(g(z))^2\,dz\quad (i,j=4,5) \tag{17}$$

In the case of transverse bending, the actions exerted are reduced to the transverse loads exerted on the faces of the laminate. The work done by applied forces can be written as

$$V=-\int_0^L q(w_b+w_s)dx \tag{18}$$

Where

q : Transverse distributed loads.

The principle of minimum total potential energy is used herein to derive the governing equation (Reddy 84). This principle can be given in analytical form as follows

$$\delta(U+V)=0 \tag{19}$$

Where

U : strain energy of the plate.

δ : indicates a variation with respect to x and y respectively.

By replacing Eqs. (11), (18) in equation (19) and integrating the equation into parts. After this integration, collecting the coefficients of δu, δv, δw_b and δw_S, the equations of motion for the orthotropic laminated plates are obtained as follows

$$\frac{\partial N_x}{\partial x}+\frac{\partial N_{xy}}{\partial y}=0 \tag{20a}$$

$$\frac{\partial N_{xy}}{\partial x}+\frac{\partial N_y}{\partial y}=0 \tag{20b}$$

$$\left[\frac{\partial^2 M_x^b}{\partial x^2}+2\frac{\partial^2 M_{xy}^b}{\partial x\partial y}+\frac{\partial^2 M_y^b}{\partial y^2}\right]+q=0 \tag{20c}$$

$$\left[\frac{\partial^2 M_x^s}{\partial x^2}+2\frac{\partial^2 M_{xy}^s}{\partial x\partial y}+\frac{\partial^2 M_y^s}{\partial y^2}+\frac{\partial Q_{xz}^s}{\partial x}+\frac{\partial Q_{yz}^s}{\partial y}\right]+q=0 \tag{20d}$$

The equilibrium equations of the refined four-variable theory of laminated plates can be expressed in terms of displacements (u, v, w_b, w_s), by introducing the forces and moment of the laminated Eqs. (13a), (13b), (13c) and (16) in relations (20a)-(20d), we obtain the fundamental relations of refined four-variable theory of laminated plates

$$A_{11}\frac{\partial^2 u}{\partial x^2}+2A_{16}\frac{\partial^2 u}{\partial x\partial y}+A_{66}\frac{\partial^2 u}{\partial y^2}+A_{16}\frac{\partial^2 v}{\partial x^2}+(A_{12}+A_{66})\frac{\partial^2 v}{\partial x\partial y}+A_{26}\frac{\partial^2 v}{\partial y^2}\\ -\left[B_{11}\frac{\partial^3 w_b}{\partial x^3}+3B_{16}\frac{\partial^3 w_b}{\partial x^2\partial y}+(B_{12}+2B_{66})\frac{\partial^3 w_b}{\partial x\partial y^2}+B_{26}\frac{\partial^3 w_b}{\partial y^3}\right]\\ -\left[B_{11}^s\frac{\partial^3 w_s}{\partial x^3}+3B_{16}^s\frac{\partial^3 w_s}{\partial x^2\partial y}+(B_{12}^s+2B_{66}^s)\frac{\partial^3 w_s}{\partial x\partial y^2}+B_{26}^s\frac{\partial^3 w_s}{\partial y^3}\right]=0 \tag{21a}$$

$$A_{16}\frac{\partial^2 u}{\partial x^2}+(A_{12}+A_{66})\frac{\partial^2 u}{\partial x\partial y}+A_{26}\frac{\partial^2 u}{\partial y^2}+A_{66}\frac{\partial^2 v}{\partial x^2}+2A_{26}\frac{\partial^2 v}{\partial x\partial y}+A_{22}\frac{\partial^2 v}{\partial y^2}\\ -\left[B_{16}\frac{\partial^3 w_b}{\partial x^3}+(B_{12}+2B_{66})\frac{\partial^3 w_b}{\partial x^2\partial y}+3B_{26}\frac{\partial^3 w_b}{\partial x\partial y^2}+B_{22}\frac{\partial^3 w_b}{\partial y^3}\right]\\ -\left[B_{16}^s\frac{\partial^3 w_s}{\partial x^3}+(B_{12}^s+2B_{66}^s)\frac{\partial^3 w_s}{\partial x^2\partial y}+3B_{26}^s\frac{\partial^3 w_s}{\partial x\partial y^2}+B_{22}^s\frac{\partial^3 w_s}{\partial y^3}\right]=0 \tag{21b}$$

$$B_{11}\frac{\partial^3 u}{\partial x^3}+3B_{16}\frac{\partial^3 u}{\partial x^2\partial y}+(B_{12}+2B_{66})\frac{\partial^3 u}{\partial x\partial y^2}+B_{26}\frac{\partial^3 u}{\partial y^3}+B_{16}\frac{\partial^3 v}{\partial x^3}\\ +(B_{12}+2B_{66})\frac{\partial^3 v}{\partial x^2\partial y}+3B_{26}\frac{\partial^3 v}{\partial x\partial y^2}+B_{22}\frac{\partial^3 v}{\partial y^3}\\ -\left[D_{11}\frac{\partial^4 w_b}{\partial x^4}+4D_{16}\frac{\partial^4 w_b}{\partial x^3\partial y}+2(D_{12}+2D_{66})\frac{\partial^4 w_b}{\partial x^2\partial y^2}\right.\\ \left.+4D_{26}\frac{\partial^4 w_b}{\partial x\partial y^3}+D_{22}\frac{\partial^4 w_b}{\partial y^4}\right]\\ -\left[D_{11}^s\frac{\partial^4 w_s}{\partial x^4}+4D_{16}^s\frac{\partial^4 w_s}{\partial x^3\partial y}+2(D_{12}^s+2D_{66}^s)\frac{\partial^4 w_s}{\partial x^2\partial y^2}\right.\\ \left.+4D_{26}^s\frac{\partial^4 w_s}{\partial x\partial y^3}+D_{22}^s\frac{\partial^4 w_s}{\partial y^4}\right]+q=0 \tag{21c}$$

$$
\begin{aligned}
&B_{11}^{s}\frac{\partial^3 u}{\partial x^3}+3B_{16}^{s}\frac{\partial^3 u}{\partial x^2\partial y}+(B_{12}^{s}+2B_{66}^{s})\frac{\partial^3 u}{\partial x\partial y^2}+B_{26}^{s}\frac{\partial^3 u}{\partial y^3}\\
&+B_{16}^{s}\frac{\partial^3 v}{\partial x^3}+(B_{12}^{s}+2B_{66}^{s})\frac{\partial^3 v}{\partial x^2\partial y}+3B_{26}^{s}\frac{\partial^3 v}{\partial x\partial y^2}\\
&+B_{22}^{s}\frac{\partial^3 v}{\partial y^3}-\left[D_{11}^{s}\frac{\partial^4 w_b}{\partial x^4}+4D_{16}^{s}\frac{\partial^4 w_b}{\partial x^3\partial y}\right.\\
&\left.+2(D_{12}^{s}+2D_{66}^{s})\frac{\partial^4 w_b}{\partial x^2\partial y^2}+4D_{26}^{s}\frac{\partial^4 w_b}{\partial x\partial y^3}+D_{22}^{s}\frac{\partial^4 w_b}{\partial y^4}\right]\\
&-\left[H_{11}^{s}\frac{\partial^4 w_s}{\partial x^4}+4H_{16}^{s}\frac{\partial^4 w_s}{\partial x^3\partial y}+2(H_{12}^{s}+2H_{66}^{s})\frac{\partial^4 w_s}{\partial x^2\partial y^2}+4H_{26}^{s}\frac{\partial^4 w_s}{\partial x\partial y^3}\right.\\
&\left.+H_{22}^{s}\frac{\partial^4 w_s}{\partial y^4}\right]+A_{55}^{s}\frac{\partial^2 w_s}{\partial x^2}+A_{44}^{s}\frac{\partial^2 w_s}{\partial y^2}+2A_{45}^{s}\frac{\partial^2 w_s}{\partial x\partial y}+q=0
\end{aligned} \tag{21d}
$$

or, more concisely

$$
\begin{bmatrix} L_{11} & L_{12} & L_{13} & L_{14}\\ L_{12} & L_{22} & L_{23} & L_{24}\\ L_{13} & L_{23} & L_{33} & L_{34}\\ L_{14} & L_{24} & L_{34} & L_{44}\end{bmatrix}\begin{Bmatrix} u\\ v\\ w_b\\ w_s\end{Bmatrix}=\begin{Bmatrix}0\\0\\q\\q\end{Bmatrix} \tag{22}
$$

With

$$
\begin{aligned}
&L_{11}=A_{11}\nabla_{xx}+2A_{16}\nabla_{xy}+A_{66}\nabla_{yy};\\
&L_{12}=A_{16}\nabla_{xx}+(A_{12}+A_{66})\nabla_{xy}+A_{26}\nabla_{yy}\\
&L_{13}=-B_{11}\nabla_{xxx}-3B_{16}\nabla_{xxy}-(B_{12}+2B_{66})\nabla_{xyy}-B_{26}\nabla_{yyy};\\
&L_{14}=-B_{11}^{s}\nabla_{xxx}-3B_{16}^{s}\nabla_{xxy}-(B_{12}^{s}+2B_{66}^{s})\nabla_{xyy}-B_{26}^{s}\nabla_{yyy}\\
&L_{22}=A_{66}\nabla_{xx}+2A_{26}\nabla_{xy}+A_{22}\nabla_{yy};\\
&L_{23}=-B_{16}\nabla_{xxx}-(B_{12}+2B_{66})\nabla_{xxy}-3B_{26}\nabla_{xyy}-B_{22}\nabla_{yyy}\\
&L_{24}=-B_{16}^{s}\nabla_{xxx}+(B_{12}^{s}+2B_{66}^{s})\nabla_{xxy}+3B_{26}^{s}\nabla_{xyy}+B_{22}^{s}\nabla_{yyy}\\
&L_{33}=D_{11}+4D_{16}\nabla_{xxxy}+2(D_{12}+2D_{66})\nabla_{xxyy}+4D_{26}\nabla_{xyyy}+D_{22}\nabla_{yyyy}\\
&L_{34}=D_{11}^{s}\nabla_{xxxx}+4D_{16}^{s}\nabla_{xxxy}+2(D_{12}^{s}+2D_{66}^{s})\nabla_{xxyy}+4D_{26}^{s}\nabla_{xyyy}+D_{22}^{s}\nabla_{yyyy}\\
&L_{44}=H_{11}^{s}\nabla_{xxxx}+4H_{16}^{s}\nabla_{xxxy}+2(H_{12}^{s}+2H_{66}^{s})\nabla_{xxyy}4H_{26}^{s}\nabla_{xyyy}\\
&+H_{22}^{s}\nabla_{yyyy}-A_{55}^{s}\nabla_{xx}-A_{44}^{s}\nabla_{yy}-2A_{45}^{s}\nabla_{xy}
\end{aligned} \tag{23}
$$

In addition

$$
\begin{aligned}
&\nabla_{xx}=\frac{\partial^2}{\partial x^2};\nabla_{xxx}=\frac{\partial^3}{\partial x^3};\nabla_{xxxx}=\frac{\partial^4}{\partial x^4};\nabla_{yy}=\frac{\partial^2}{\partial y^2};\\
&\nabla_{yyy}=\frac{\partial^3}{\partial y^3};\nabla_{yyyy}=\frac{\partial^4}{\partial y^4}\nabla_{xy}=\frac{\partial^2}{\partial x\partial y};\nabla_{xxy}=\frac{\partial^3}{\partial x^2\partial y}\\
&\nabla_{xyy}=\frac{\partial^3}{\partial x\partial y^2};\nabla_{xxyy}=\frac{\partial^4 w_b}{\partial x^2\partial y^2};\nabla_{xxxy}=\frac{\partial^4}{\partial x^3\partial y};\nabla_{xyyy}=\frac{\partial^4}{\partial x\partial y^3}
\end{aligned} \tag{24}
$$

2.2.1.5 Analytical solutions

2.2.1.5.1 Antisymmetric cross-ply laminates

For antisymmetric cross-ply laminates plates, the following terms of plate stiffness are null

$$
\begin{aligned}
A_{16}&=A_{26}=D_{16}=D_{26}=D_{16}^{s}=D_{26}^{s}=F_{16}\\
&=F_{26}=H_{16}=H_{26}=H_{16}^{s}=H_{26}^{s}=0\\
B_{12}&=B_{16}=B_{26}=B_{66}=B_{12}^{s}=B_{16}^{s}=B_{26}^{s}\\
&=B_{66}^{s}=E_{12}=E_{16}=E_{26}=E_{66}=0
\end{aligned}
$$

$$
\begin{aligned}
&A_{45}=A_{45}^{a}=A_{45}^{s}=D_{45}=F_{45}=0\\
&B_{22}=-B_{11};\quad B_{22}^{s}=-B_{11}^{s};\quad E_{22}=-E_{11}
\end{aligned} \tag{25}
$$

To solve the system of Eq. (21), we use the method of Navier. It is assumed that the displacements u,v,w_b,w_s are written in the following form in order to satisfy the boundary conditions

$$
\begin{aligned}
u(x,y)&=\sum_{m=1}^{\infty}\sum_{n=1}^{\infty}U_{mn}\cos\alpha x\sin\beta y\\
v(x,y)&=\sum_{m=1}^{\infty}\sum_{n=1}^{\infty}V_{mn}\sin\alpha x\cos\beta y\\
w_b(x,y)&=\sum_{m=1}^{\infty}\sum_{n=1}^{\infty}W_{b\,mn}\sin\alpha x\sin\beta y\\
w_s(x,y)&=\sum_{m=1}^{\infty}\sum_{n=1}^{\infty}W_{s\,mn}\sin\alpha x\sin\beta y
\end{aligned} \tag{26}
$$

To solve this problem, Navier introduced the external force as a double trigonometric series.

$$
q(x,y)=\sum_{m=1}^{\infty}\sum_{n=1}^{\infty}q_{mn}\sin\alpha x\cos\beta y \tag{27}
$$

Where

$\alpha=m\pi/a;\ \beta=n\pi/b$

The two types of sinusoidal r uniform distributed loads to which the plate is subjected are given by the following expressions

$$
\begin{aligned}
&Q_{mn}=q && \text{Sinusoidal load}\\
&Q_{mn}=\frac{16q}{mn^2} && \text{Uniformly load}
\end{aligned} \tag{28}
$$

Substitute the Eqs. (24), (25) and (26) in the system of Eq. (21), we obtain the following system of equations

$$
\begin{bmatrix} s_{11} & s_{12} & s_{13} & s_{14}\\ s_{12} & s_{22} & s_{23} & s_{24}\\ s_{13} & s_{23} & s_{33} & s_{34}\\ s_{14} & s_{24} & s_{34} & s_{44}\end{bmatrix}\begin{Bmatrix} U_{mn}\\ V_{mn}\\ W_{bmn}\\ W_{smn}\end{Bmatrix}=\begin{Bmatrix}0\\0\\Q_{mn}\\Q_{mn}\end{Bmatrix} \tag{29}
$$

Where

$$
\begin{aligned}
&s_{11}=A_{11}\alpha^2+A_{66}\beta^2,\quad s_{12}=\alpha\beta(A_{12}+A_{66}),\\
&s_{13}=-B_{11}\alpha^3,\quad s_{14}=-B_{11}^{s}\alpha^3,\\
&s_{22}=A_{66}\alpha^2+A_{22}\beta^2\\
&s_{23}=B_{11}\beta^3,\quad s_{24}=B_{11}^{s}\beta^3,\\
&s_{33}=D_{11}\alpha^4+2(D_{12}+2D_{66})\alpha^2\beta^2+D_{22}\beta^4\\
&s_{34}=D_{11}^{s}\alpha^4+2(D_{12}^{s}+2D_{66}^{s})\alpha^2\beta^2+D_{22}^{s}\beta^4\\
&s_{44}=H_{11}^{s}\alpha^4+2(H_{12}^{s}+2H_{66}^{s})\alpha^2\beta^2+H_{22}^{s}\beta^4+A_{55}^{s}\alpha^2+A_{44}^{s}\beta^2
\end{aligned} \tag{30}
$$

According to the Eqs (29) and (30), the generalized displacements can be solved. The stresses of the rectangular laminated composite can then be obtained from the Eqs. (4a), (4b), (6a) and (6b), as follows

$$
\begin{Bmatrix}\sigma_x\\ \sigma_y\\ \sigma_{xy}\end{Bmatrix}^{(k)}=\sum_{n;m}\left\langle\begin{bmatrix}\bar{Q}_{11} & \bar{Q}_{12} & \bar{Q}_{16}\\ \bar{Q}_{12} & \bar{Q}_{26} & \bar{Q}_{26}\\ \bar{Q}_{16} & \bar{Q}_{26} & \bar{Q}_{66}\end{bmatrix}^{(k)}\right.
$$

$$\times\left\{\begin{matrix}\left(-\alpha U_{mn}-z\alpha^2 W_{bmn}-\alpha^2 f(z) W_{smn}\right)\sin\alpha x\sin\beta y\\ \left(-\beta U_{mn}-z\beta^2 W_{bmn}-\beta^2 f(z) W_{smn}\right)\sin\alpha x\sin\beta y\\ \left((\alpha+\beta) U_{mn} z-2(\alpha+\beta)\alpha^2 W_{bmn}-2(\alpha+\beta) f(z) W_{smn}\right)\cos\alpha x\cos\beta y\end{matrix}\right\}\Bigg\rangle \tag{31a}$$

$$\begin{Bmatrix}\sigma_{yz}\\ \sigma_{xz}\end{Bmatrix}^{(k)}=\sum_{m,n}\left\langle\begin{bmatrix}\bar{Q}_{44} & \bar{Q}_{45}\\ \bar{Q}_{45} & \bar{Q}_{55}\end{bmatrix}^{(k)} g(z)\begin{Bmatrix}\alpha W_{smn}\cos\alpha x\sin\beta y\\ \beta W_{smn}\sin\alpha x\cos\beta y\end{Bmatrix}\right\rangle \tag{31b}$$

2.2.1.5.2 Antisymmetric angle-ply laminates

For antisymmetric angle-ply laminates, the following terms of plate stiffness are null

$$\begin{aligned}&A_{16}=A_{26}=D_{16}=D_{26}=D_{16}^s=D_{26}^s=F_{16}\\ &=F_{26}=H_{16}=H_{26}=H_{16}^s=H_{26}^s=0\\ &B_{11}=B_{12}=B_{22}=B_{66}=B_{11}^s=B_{12}^s=B_{22}^s\\ &=B_{66}^s=E_{11}=E_{12}=E_{22}=E_{66}=0\\ &A_{45}=A_{45}^a=A_{45}^s=D_{45}=F_{45}=0;\end{aligned} \tag{32}$$

To solve the Eq. (21), one uses the method of Navier. It is assumed that the displacements u, v, w_b, w_s are written in the following form in order to satisfy the boundary conditions

$$\begin{aligned}u(x,y)&=\sum_{m=1}^{\infty}\sum_{n=1}^{\infty}U_{mn}\sin\alpha x\cos\beta y\\ v(x,y)&=\sum_{m=1}^{\infty}\sum_{n=1}^{\infty}V_{mn}\cos\alpha x\sin\beta y\\ w_b(x,y)&=\sum_{m=1}^{\infty}\sum_{n=1}^{\infty}W_{bmn}\sin\alpha x\sin\beta y\\ w_s(x,y)&=\sum_{m=1}^{\infty}\sum_{n=1}^{\infty}W_{smn}\sin\alpha x\sin\beta y\end{aligned} \tag{33}$$

Substitute the Eqs. (32) and (33) in the system of Eq. (21), we obtain the system of Eq. (29) with the following coefficients:

$$\begin{aligned}&s_{11}=A_{11}\alpha^2+A_{66}\beta^2,\quad s_{12}=\alpha\beta(A_{12}+A_{66}),\\ &s_{13}=-(3B_{16}\alpha^2\beta+B_{26}\beta^3),\quad s_{14}=-(3B_{16}^s\alpha^2\beta+B_{26}^s\beta^3)\\ &s_{22}=A_{66}\alpha^2+A_{22}\beta^2,\quad s_{23}=-(B_{16}\alpha^3+3B_{26}\alpha\beta^2),\\ &s_{24}=-(B_{16}^s\alpha^3+3B_{26}^s\alpha\beta^2)\\ &s_{33}=D_{11}\alpha^4+2(D_{12}+2D_{66})\alpha^2\beta^2+D_{22}\beta^4\\ &s_{34}=D_{11}^s\alpha^4+2(D_{12}^s+2D_{66}^s)\alpha^2\beta^2+D_{22}^s\beta^4\\ &s_{44}=H_{11}^s\alpha^4+2(H_{12}^s+2H_{66}^s)\alpha^2\beta^2+H_{22}^s\beta^4+A_{55}^s\alpha^2+A_{44}^s\beta^2\end{aligned} \tag{34}$$

Stresses of the rectangular laminated composite can then be obtained from the equations. (4a), (4b), (6a) and (6b), as follows

$$\begin{Bmatrix}\sigma_x\\ \sigma_y\\ \sigma_{xy}\end{Bmatrix}^{(k)}=\sum_{n;m}\left\langle\begin{bmatrix}\bar{Q}_{11} & \bar{Q}_{12} & \bar{Q}_{16}\\ \bar{Q}_{12} & \bar{Q}_{26} & \bar{Q}_{26}\\ \bar{Q}_{16} & \bar{Q}_{26} & \bar{Q}_{66}\end{bmatrix}^{(k)}\right.$$

$$\times\left\{\begin{matrix}\left(-\alpha U_{mn}-z\alpha^2 W_{bmn}-\alpha^2 f(z) W_{smn}\right)\sin\alpha x\sin\beta y\\ \left(-\beta U_{mn}-z\beta^2 W_{bmn}-\beta^2 f(z) W_{smn}\right)\sin\alpha x\sin\beta y\\ \left((\alpha+\beta) U_{mn} z-2(\alpha+\beta)\alpha^2 W_{bmn}-2(\alpha+\beta) f(z) W_{smn}\right)\cos\alpha x\cos\beta y\end{matrix}\right\}\Bigg\rangle \tag{35a}$$

Table 1 Mechanical properties of materials

Materials	E_1	G_{12}	G_{13}	G_{23}	v_{12}
Material 1[a]	$25E_2$	$0.5E_2$	$0.5E_2$	$0.2E_2$	0.25
Material 2[b]	$40E_2$	$0.6E_2$	$0.6E_2$	$0.5E_2$	0.25

[a]Pagano 70; [b]Noor 75

$$\begin{Bmatrix}\sigma_{yz}\\ \sigma_{xz}\end{Bmatrix}^{(k)}=\sum_{m,n}\left\langle\begin{bmatrix}\bar{Q}_{44} & \bar{Q}_{45}\\ \bar{Q}_{45} & \bar{Q}_{55}\end{bmatrix}^{(k)} g(z)\begin{Bmatrix}\alpha W_{smn}\cos\alpha x\sin\beta y\\ \beta W_{smn}\sin\alpha x\cos\beta y\end{Bmatrix}\right\rangle \tag{35b}$$

3. Results and interpretations

In the first step, based on mathematical formulations, a computer program is developed to study the behavior of orthotropic, symmetric cross-ply, antisymmetric cross-ply and antisymmetric angle-ply laminated symmetric plates with simply supported edges using the refined four-variable plate theory. The mechanical characteristics of the materials used summarized in Table 1.

The numerical results of deflections and stress are given in dimensionless form

$$\begin{aligned}&\bar{W}=W(x,y)\left(\frac{E_2h^3}{b^4q}\right),\quad \bar{\sigma}_x=\sigma_x(a/2,b/2,z)\left(\frac{h^2}{b^2q}\right),\\ &\bar{\sigma}_y=\sigma_y(a/2,b/2,z)\left(\frac{h^2}{b^2q}\right),\ \bar{\sigma}_{xy}=\sigma_{xy}(a,b,z)\left(\frac{h^2}{b^2q}\right),\\ &\bar{\sigma}_{xz}=\sigma_{xz}(0,b/2,z)\left(\frac{h}{bq}\right),\quad \bar{\sigma}_{yz}=\sigma_{xz}(a/2,0,z)\left(\frac{h}{bq}\right),\end{aligned} \tag{36}$$

3.1 Comparison of results

3.1.1 Orthotropic square plates and symmetric cross-ply laminated plates

In the first part, we are interested in validating the results of orthotropic square plates and symmetric cross-ply laminated plates of stacking sequences (0°/90°/0°) and (0°/90°/90°/0°) obtained by the four variables refined theory by resulted available in literature. The plates have simply supported subjected to uniform (CU) or sinusoidal distributed loads (CDS), respectively. The tests are performed for different geometric ratio values (a/h=10, 20 and 100) for the CDS load and geometric ratio values (a/h=10 and 100) for the CU load. Material 1 is used. The results are presented in Tables 2, 3,4 and 5.

From the Tables 2-5, we can see that the results obtained by the present theory RPT are close to those obtained by the FSDT theory. The theory involves four unknown variables, as against five in case of first-order shear deformation theory. The theory gives rise to transverse shear stress variation such that the transverse shear stresses vary parabolically across the thickness satisfying shear stress free conditions at top and bottom surfaces of the plate. The theory does not require problem-dependent shear correction factors that are associated with the first-order shear deformation theory.

Table 6 presented the nondimensionalized deflections of

Table 2 Comparison of the results of nondimensionalized deflections and maximum nondimensionalized stresses. Case of simply supported orthotropic square plates subjected to sinusoidal distributed loads (Material 1)

a/h	Theories	$\overline{w}$	$\overline{\sigma}_x$	$\overline{\sigma}_y$	$\overline{\sigma}_{xy}$
10	FSDT[a]	0.6383	0.5248	0.0339	0.0246
	Present (*n*=3)	0.6041	0.5747	0.0284	0.0227
	Present (*n*=5)	0.6011	0.5652	0.0280	0.0280
	Present (*n*=7)	0.5971	0.5594	0.0277	0.0277
	Present (*n*=9)	0.5939	0.5556	0.0275	0.0275
20	FSDT[a]	0.4836	0.5350	0.0286	0.0222
	Present (*n*=3)	0.4746	0.5477	0.0271	0.0216
	Present (*n*=5)	0.4738	0.5453	0.0270	0.0280
	Present (*n*=7)	0.4727	0.5439	0.0269	0.0277
	Present (*n*=9)	0.4719	0.5429	0.0269	0.0275
100	FSDT[a]	0.4333	0.5385	0.0267	0.0213
	Present (*n*=3)	0.4330	0.5391	0.0267	0.0213
	Present (*n*=5)	0.4329	0.5390	0.0267	0.0280
	Present (*n*=7)	0.4329	0.5389	0.0267	0.0277
	Present (*n*=9)	0.4329	0.5389	0.0267	0.0275
	CLPT[a]	0.4312	0.5387	0.0267	0.0213

[a]Reddy 2004

Table 3 Comparison of the results of nondimensionalized deflections and maximum nondimensionalized stresses. Case of simply supported orthotropic square plates subjected a uniform load (Material 1)

a/h	Theories	Orthotrope	($0^0/90^0/0^0$)	($0^0/90^0/90^0/0^0$)
10	FSDT[a]	0.9519	1.0219	1.0219
	Present (*n*=3)	0.8976	0.9159	0.9280
	Present (*n*=5)	0.8931	0.9123	0.9252
	Present (*n*=7)	0.8872	0.9066	0.9200
	Present (*n*=9)	0.8826	0.9021	0.9156
	ANSYS	0.9671	1.0373	1.0392
100	FSDT[a]	0.6528	0.6697	0.6833
	Present (*n*=3)	0.6522	0.6685	0.6822
	Present (*n*=5)	0.6522	0.6685	0.6821
	Present (*n*=7)	0.6521	0.6684	0.6821
	Present (*n*=9)	0.6521	0.6684	0.6820
	ANSYS	0.6540	0.6710	0.6847

[a]Reddy 2004

simply supported three-layer square laminates of three-layer (450/30°/60°) and (45°/30°/90°) under sinusoidal transverse load with various span-to-thickness ratios (*a/h*=5,10,20 and 100). It is noted that for thick plates (*L/h*=5) and for thin plates (*a/h*=100). Material set 1 is used. The theory is variationally consistent and avoids the need of shear correction factors.

Figs. 5 and 6 show the stacking of the layers of the laminated plates simulated on computation software of structures Ansys 12.

In the following, we present in Figs. 7-12, the *Z*-axis displacement of the orthotropic square plates and symmetrical cross-ply laminated square plates of type (00/900/00), (00/900/900/00), respectively. These results obtained using the finite element method for *a/h*=10,100. The values of the deflections also exist in Table 5 in the nondimensionalized form. Symmetric laminates are thus

Table 4 Comparison of the results of nondimensionalized deflections and maximum nondimensionalized stresses. Case of simply supported three-layered antisymmetric cross-ply square laminate plates ($0^0/90^0/0^0$) subjected to doubly sinusoidal distributed loads (Material 1)

a/h	Theories	$\overline{W}$	$\overline{\sigma}_x$	$\overline{\sigma}_y$	$\overline{\sigma}_{xy}$	$\overline{\sigma}_{xz}$	$\overline{\sigma}_{yz}$
10	FSDT[a]	0.6693	0.5134	0.2536	0.0252	0.4089	0.1936
	Present (*n*=3)	0.6041	0.5747	0.1649	0.0227	0.3017	0.3017
	Present (*n*=5)	0.6011	0.5652	0.1731	0.0223	0.2882	0.2882
	Present (*n*=7)	0.5971	0.5594	0.1761	0.0221	0.2731	0.2731
	Present (*n*=9)	0.5939	0.5556	0.1775	0.0219	0.2634	0.2634
20	FSDT[a]	0.4921	0.5318	0.1997	0.0223	0.4205	0.1805
	Present (*n*=3)	0.4746	0.5477	0.1759	0.0216	0.3028	0.3028
	Present (*n*=5)	0.4738	0.5453	0.1780	0.0215	0.2886	0.2886
	Present (*n*=7)	0.4727	0.5439	0.1787	0.0215	0.2733	0.2733
	Present (*n*=9)	0.4719	0.5429	0.1790	0.0214	0.2635	0.2635
100	FSDT[a]	0.4337	0.5384	0.1804	0.0213	0.4247	0.1746
	Present (*n*=3)	0.4330	0.5391	0.1794	0.0213	0.3031	0.3031
	Present (*n*=5)	0.4329	0.5390	0.1795	0.0213	0.2887	0.2887
	Present (*n*=7)	0.4329	0.5389	0.1795	0.0213	0.2733	0.2733
	Present (*n*=9)	0.4329	0.5389	0.1795	0.0213	0.2635	0.2635
	CLPT[a]	0.4312	0.5387	0.1796	0.0213	--	--

[a]Reddy 2004

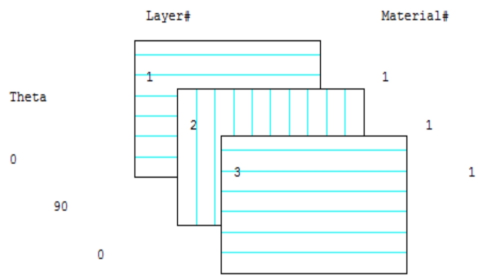

Fig. 5 Stacking layers of symmetric cross-ply laminated of type (0°/90°/0°)

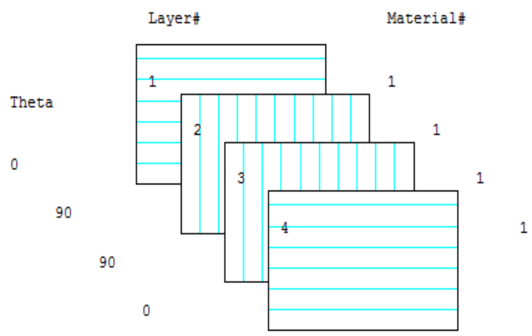

Fig.6 Stacking layers of symmetric cross-ply laminated of type (0°/90°/90°/0°)

Table 5 Comparison of the results of nondimensionalized deflections and maximum nondimensionalized stresses. Case of simply supported four-layered symmetric cross-ply square laminate plates ($0^0/90^0/90^0/0^0$) subjected to doubly sinusoidal distributed loads (Material 1)

a/h	Theories	$\overline{W}$	$\bar{\sigma}_x$	$\bar{\sigma}_y$	$\bar{\sigma}_{xy}$	$\bar{\sigma}_{xz}$	$\bar{\sigma}_{yz}$
10	FSDT[a]	0.6693	0.5134	0.2536	0.0252	0.4089	0.1936
	Present (*n*=3)	0.6041	0.5747	0.1649	0.0227	0.3017	0.3017
	Present (*n*=5)	0.6011	0.5652	0.1731	0.0223	0.2882	0.2882
	Present (*n*=7)	0.5971	0.5594	0.1761	0.0221	0.2731	0.2731
	Present (*n*=9)	0.5939	0.5556	0.1775	0.0219	0.2634	0.2634
20	FSDT[a]	0.4921	0.5318	0.1997	0.0223	0.4205	0.1805
	Present (*n*=3)	0.4746	0.5477	0.1759	0.0216	0.3028	0.3028
	Present (*n*=5)	0.4738	0.5453	0.1780	0.0215	0.2886	0.2886
	Present (*n*=7)	0.4727	0.5439	0.1787	0.0215	0.2733	0.2733
	Present (*n*=9)	0.4719	0.5429	0.1790	0.0214	0.2635	0.2635
100	FSDT[a]	0.4337	0.5384	0.1804	0.0213	0.4247	0.1746
	Present (*n*=3)	0.4330	0.5391	0.1794	0.0213	0.3031	0.3031
	Present (*n*=5)	0.4329	0.5390	0.1795	0.0213	0.2887	0.2887
	Present (*n*=7)	0.4329	0.5389	0.1795	0.0213	0.2733	0.2733
	Present (*n*=9)	0.4329	0.5389	0.1795	0.0213	0.2635	0.2635
	CLPT[a]	0.4312	0.5387	0.1796	0.0213	--	--

[a]Reddy 2004

largely used, unless some specific conditions require nonsymmetric laminates.

3.1.1.2 Antisymmetric laminates

In this part, we see very interesting to validate the results of Nondimensionalized deflections and the maximum stresses of the antisymmetric laminated plates of stacking sequences ($0^0/90^0$) et ($0^0/90^0$)$_4$ by results available in literatures, for different geometrical ratios (*a/h*=10,20,100).

Table 6 Nondimensionalized deflections of simply supported three-layer square laminates under sinusoidal transverse load (Material 1)

Theory	($45^0/30^0/60^0$)				($45^0/30^0/90^0$)			
	a/h				*a/h*			
	5	10	20	100	5	10	20	100
Present (*n*=3)	0.9364	0.4375	0.3090	0.2675	0.9955	0.4916	0.3624	0.3208
Present (*n*=5)	0.9374	0.4352	0.3082	0.2675	0.9931	0.4888	0.3615	0.3207
Present (*n*=7)	0.9253	0.4313	0.3072	0.2675	0.9797	0.4847	0.3605	0.3207
Present (*n*=9)	0.9142	0.4283	0.3064	0.2674	0.9681	0.4816	0.3597	0.3207

The results of Tables 7 and 8, show that the nondimensionalized deflections and nondimensionalized stress obtained by the CLPT theory are independent of geometric ratio (*a/h*), while the nondimensionalized deflection values and stresses obtained by the present theory and the FSDT theory depend on geometric ratio (*a/h*), this variation explains the deformation effect of the transverse shear. It is also observed that the deformation effect of the transverse shear causes an increase of the nondimensionalized deflections in the center of the plate.

Still according to the preceding Tables, the difference between the present theory and the classical laminate plate theory concerning the nondimensionalized deflections at the center of the plate decreases when the geometric ratio (*a/h*) increases. For example, for eight-layer cross-ply square laminated plates under a sinusoidal distributed loads of geometric ratio (*a/h*=10), the difference between the present theory and the first-order shear deformation theory is about 0.21%, while for a geometric ratio (*a/h*=20), it is only 0.10%. In the case of an isotropic plate there is no coupling

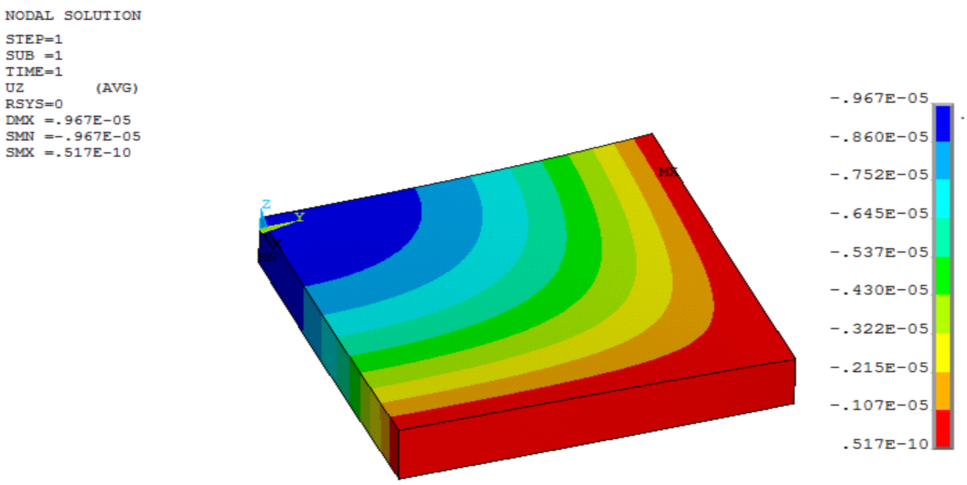

Fig. 7 Displacement following the *Z*-axis of a simply supported orthotropic plate subjected to a uniform load, Material 1, Shel99 element, *a/h*=10

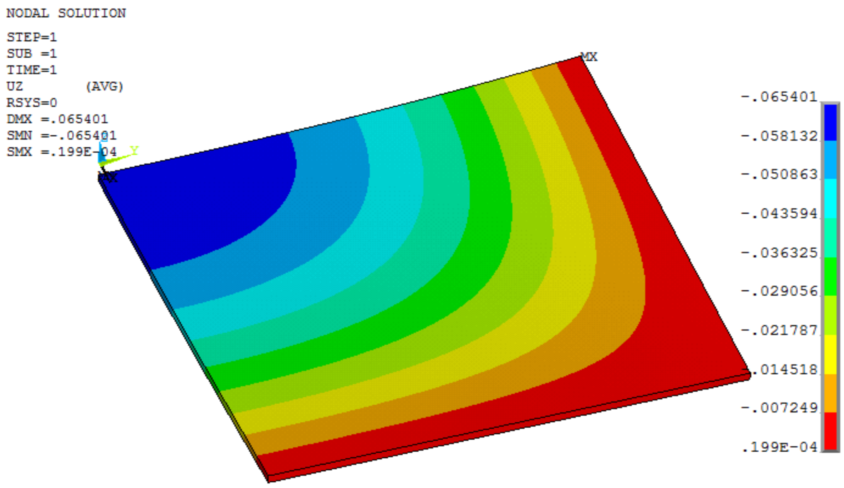

Fig. 8 Displacement following the *Z*-axis of a simply supported orthotropic plate subjected to a uniform load, Material 1, Shel99 element, *a*/*h*=100

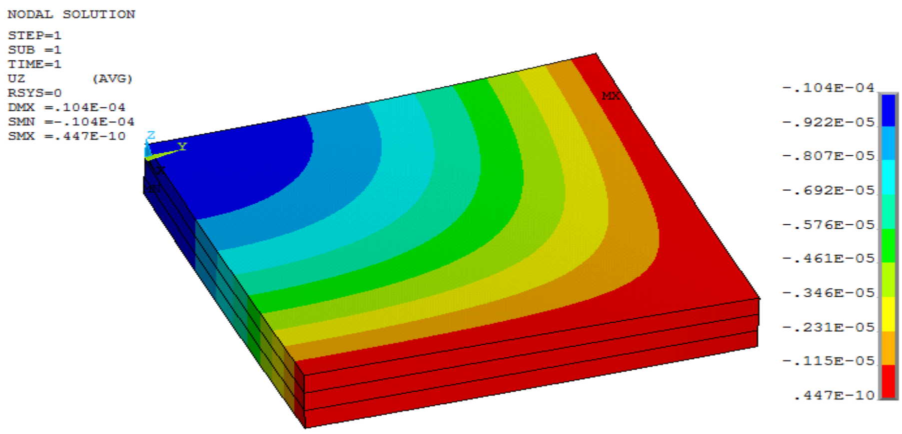

Fig. 9 Displacement following the *Z*-axis of a simply supported cross-ply laminated plate (0°/90°/0°) subjected to a uniform load, Material 1, Shel99 element, *a*/*h*=10

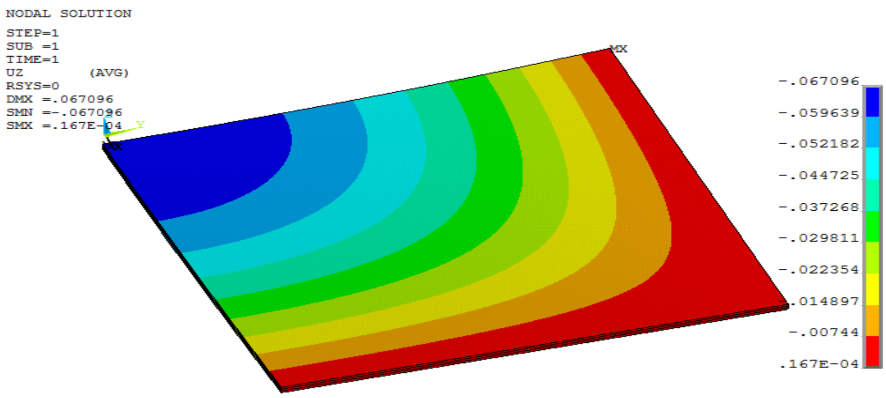

Fig. 10 Displacement following the *Z*-axis of a simply supported cross-ply laminated plate (0°/90°/0°) subjected to a uniform load, Material 1, Shel99 element, *a*/*h*=100

between in-plane behaviour and flexural behaviour of the plate. For an orthotropic layer of thickness, the material directions of which are the same as the reference directions of the plate (the reference directions of the stresses and strains applied to the plate), as in the case of an isotropic plate, the in-plane resultants depend only on the in-plane strains and the moments depend only on the curvatures.

5. Conclusions

In the first part of this paper, we presented a theory of laminated plates belonging to the family of shear models and the equivalent monolayer approach family of multilayer composites modeling. In the second part, a computer code under Matlab based on the refined four-variable theory was

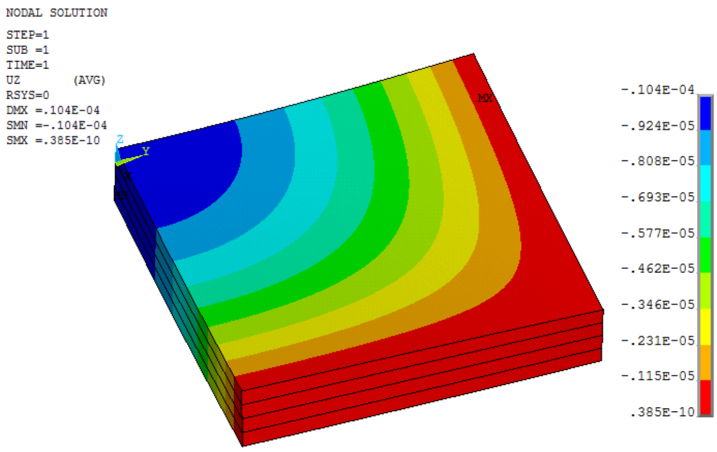

Fig. 11 Displacement following the *Z*-axis of a simply supported cross-ply laminated plate (0°/90°/90°/0°) subjected to a uniform load, Material 1, Shel99 element, *a*/*h*=10

Table 7 Comparison of the results of nondimensionalized deflections and maximum nondimensionalized stresses. Case of simply supported two-layered antisymmetric cross-ply square laminate plates ($0^0/90^0$) subjected to doubly sinusoidal distributed loads (Material 1)

a/h	Theories	$\overline{W}$	$\bar{\sigma}_x$	$\bar{\sigma}_y$	$\bar{\sigma}_{xy}$	$\bar{\sigma}_{xz}$	$\bar{\sigma}_{yz}$
10	FSDT[a]	1.2373	0.7157	0.7157	0.0525	0.2728	0.2728
	Present (*n*=3)	1.2161	0.7468	0.7468	0.0533	0.3190	0.3190
	Present (*n*=5)	1.2233	0.7401	0.7401	0.0533	0.2830	0.2830
	Present (*n*=7)	1.2234	0.7352	0.7352	0.0531	0.2685	0.2685
	Present (*n*=9)	1.2223	0.7319	0.7319	0.0530	0.2602	0.2602
20	FSDT[a]	1.1070	0.7157	0.7157	0.0525	0.2728	0.2728
	Present (*n*=3)	1.1018	0.7235	0.7235	0.0527	0.3199	0.3199
	Present (*n*=5)	1.1035	0.7218	0.7218	0.0527	0.2833	0.2833
	Present (*n*=7)	1.1035	0.7206	0.7206	0.0526	0.2686	0.2686
	Present (*n*=9)	1.1033	0.7198	0.7198	0.0526	0.2603	0.2603
100	FSDT[a]	1.0653	0.7157	0.7157	0.0525	0.2728	0.2728
	Present (*n*=3)	1.0651	0.7161	0.7161	0.0525	0.3202	0.3202
	Present (*n*=5)	1.0652	0.7160	0.7160	0.0525	0.2834	0.2834
	Present (*n*=7)	1.0652	0.7159	0.7159	0.0525	0.2687	0.2687
	Present (*n*=9)	1.0652	0.7159	0.7159	0.0525	0.2603	0.2603
	CLPT[a]	1.0636	0.7157	0.7157	0.0525	--	--

[a]Reddy 2004

Table 8 Comparison of the results of nondimensionalized deflections and maximum nondimensionalized stresses. Case of simply supported eight-layered antisymmetric cross-ply square laminate plates $(0^0/90^0)_4$ subjected to doubly sinusoidal distributed loads (Material 1)

a/h	Theories	$\overline{W}$	$\bar{\sigma}_x$	$\bar{\sigma}_y$	$\bar{\sigma}_{xy}$	$\bar{\sigma}_{xz}$	$\bar{\sigma}_{yz}$
10	FSDT[a]	0.6216	0.4950	0.4950	0.0221	0.2728	0.2728
	Present (*n*=3)	0.6229	0.5285	0.5285	0.0236	0.3416	0.3416
	Present (*n*=5)	0.6191	0.5198	0.5198	0.0232	0.2930	0.2930
	Present (*n*=7)	0.6146	0.5145	0.5145	0.0229	0.2742	0.2742
	Present (*n*=9)	0.6111	0.5111	0.5111	0.0228	0.2639	0.2639
20	FSDT[a]	0.4913	0.4950	0.4950	0.0221	0.2728	0.2728
	Present (*n*=3)	0.4918	0.5034	0.5034	0.0225	0.3427	0.3427
	Present (*n*=5)	0.4907	0.5012	0.5012	0.0224	0.2934	0.2934
	Present (*n*=7)	0.4896	0.4999	0.4999	0.0223	0.2744	0.2744
	Present (*n*=9)	0.4887	0.4990	0.4990	0.0223	0.2640	0.2640
100	FSDT[a]	0.4496	0.4950	0.4950	0.0221	0..2728	0..2728
	Present (*n*=3)	0.4496	0.4953	0.4953	0.0221	0.3431	0.3431
	Present (*n*=5)	0.4496	0.4952	0.4952	0.0221	0.2935	0.2935
	Present (*n*=7)	0.4496	0.4952	0.4952	0.0221	0.2744	0.2744
	Present (*n*=9)	0.4495	0.4951	0.4951	0.0221	0.2640	0.2640
	CLPT[a]	0.4479	0.4950	0.4950	0.0221	--	--

[a]Reddy 2004

developed for the behavioral analysis of bending of orthotropic plates and laminated composite plates. Plates subjected to either doubly sinusoidal charges or uniform charge. The results obtained are compared with the results available in the bibliography and the finite element method Ansys12. After modeling, we ended up with the following results:

Composite plates are widely used in civil, mechanical, aeronautical, and especially aerospace structures. This is mainly due to their very high strength and specific rigidity and the advantage of adapting their properties to meet the requirements of the practice.

By dividing the transverse displacement into shearing parts, the number of unknowns in the theory is reduced,

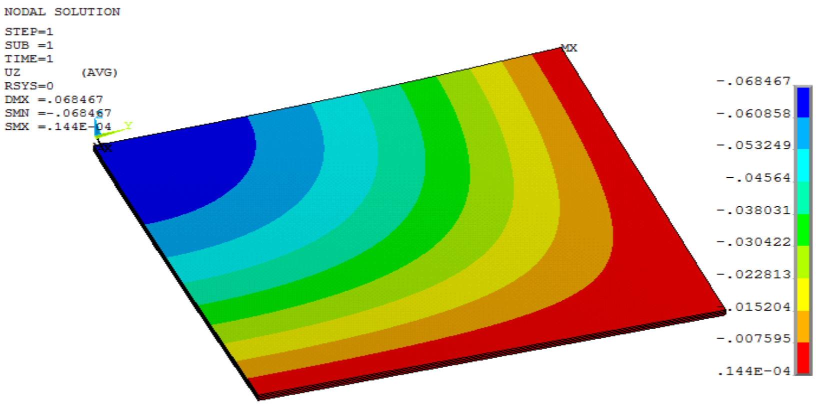

Fig. 12 Displacement following the *Z*-axis of a simply supported cross-ply laminated plate (0°/90°/90°//0°) subjected to a uniform load, Material 1, Shel99 element, *a/h*=100

which saves computing time.

The results of the sample problem show good agreement with the literature values as seen from the validation checks. It should be noted that the present theory involves only four independent variables as against five in the case of FSDT. Also, the present theory does not required shear correction factors as in the case of FSDT.

The orientation of the fibers has a great effect on the mechanical behavior of laminated composite plates.

References

Abdelmalek, A., Bouazza, M., Zidour, M. and Benseddiq, N. (2019), "Hygrothermal effects on the free vibration behavior of composite plate using nth-order shear deformation theory: a micromechanical approach", *Iran J. Sci. Technol. Tran. Mech. Eng*., **43**(1), 61-73. https://doi.org/10.1007/s40997-017-0140-y.

Ambartsumyan, S.A. (1969), *Theory of Anisotropic Plate*, Technomic Publishing.

Antar, K., Amara, K., Benyoucef, S., Bouazza, M. and Ellali, M. (2019), "Hygrothermal effects on the behavior of reinforced-concrete beams strengthened by bonded composite laminate plates", *Struct. Eng. Mech*., **69**(3), 327-334. https://doi.org/10.12989/sem.2019.69.3.327.

Aydogdu, M. (2009), "A new shear deformation theory for laminated composite plates", *Compos. Struct*., **89**, 94-101. https://doi.org/10.1016/j.compstruct.2008.07.008.

Becheri, T., Amara, K., Bouazza, M. and Benseddiq, N. (2016), "Buckling of symmetrically laminated plates using nth-order shear deformation theory with curvature effects", *Steel Compos. Struct*., **21**(6), 1347-1368. https://doi.org/10.12989/scs.2016.21.6.1347.

Belkacem, A., Tahar, H.D., Abderrezak, R., Amine, B.M., Mohamed, Z. and Boussad, A. (2018), "Mechanical buckling analysis of hybrid laminated composite plates under different boundary conditions", *Struct. Eng. Mech*., **66**(6), 761-769. https://doi.org/10.12989/sem.2018.66.6.761.

Bhimaraddi, A. and Stevens, L.K. (1984), "A higher order theory for free vibration of orthotropic, homogeneous, and laminated rectangular plates", *J. Appl. Mech*., **51**(1), 195-198. https://doi.org/10.1115/1.3167569.

Biswal, M., Sahu, S.K., Asha, A.V. and Nanda, N. (2016), "Hygrothermal effects on buckling of composite shell-experimental and FEM results",*Steel Compos. Struct*., **22**(6), 1445-1463. http://dx.doi.org/10.12989/scs.2016.22.6.1445.

Bouazza, M., Lairedj, A., Benseddiq, N. and Khalki, S. (2016), "A refined hyperbolic shear deformation theory for thermal buckling analysis of cross-ply laminated plates", *Mech. Res. Commun*., **73**, 117-126. https://doi.org/10.1016/j.mechrescom.2016.02.015.

Bouazza, M. and Zenkour, A.M. (2018), "Free vibration characteristics of multilayered composite plates in a hygrothermal environment via the refined hyperbolic theory", *Eur. Phys. J. Plus*., **133**, 217.

Bouazza, M., Kenouza, Y., Benseddiq, N. and Zenkour Ashraf, M. (2017), "A two-variable simplified nth-higher-order theory for free vibration behavior of laminated plates", *Compos Struct*., **182**, 533-541. https://doi.org/10.1016/j.compstruct.2017.09.041.

Bouhadra, A., Tounsi, A., Bousahla, A.A., Benyoucef, S. and Mahmoud, S.R. (2018), "Improved HSDT accounting for effect of thickness stretching in advanced composite plates", *Struct. Eng. Mech*., **66**(1), 61-73. https://doi.org/10.12989/sem.2018.66.1.061.

Bourada, F., Bousahla, A.A., Bourada, M., Azzaz, A., Zinata, A. and Tounsi, A. (2019), "Dynamic investigation of porous functionally graded beam using a sinusoidal shear deformation theory", *Wind Struct*., **28**(1), 19-30. https://doi.org/10.12989/was.2019.28.1.019.

Bousahla, A.A., Benyoucef, S. Tounsi, A. and Mahmoud, S.R. (2016), "On thermal stability of plates with functionally graded coefficient of thermal expansion", *Struct. Eng. Mech*., **60**(2), 313-335. http://dx.doi.org/10.12989/sem.2016.60.2.313.

Chen, X. and Xu, C. (2016), "Effect oflocal wall thinning on ratcheting behavior of pressurized 90° elbow pipe under reversed bending using finite element analysis", *Steel Compos. Struct.*, **20**(4), 703-753. https://doi.org/10.12989/scs.2018.28.3.389.

Chikh, A., Tounsi, A., Hebali, H. and Mahmoud, S.R. (2017), "Thermal buckling analysis of cross-ply laminated plates using a simplified HSDT", *Smart Struct. Syst*., **19**(3), 289-297. https://doi.org/10.12989/sss.2017.19.3.289.

El-Abbasi, N. and Meguid, S.A. (2000), "A new shell element accounting for through thickness deformation", *Comput. Meth. Appl. Mech. Eng*., **189**, 841-862. https://doi.org/10.1016/S0045-7825(99)00348-5.

Ellali, M., Amara, K., Bouazza, M. and Bourada, F. (2018), "The buckling of piezoelectric plates on Pasternak elastic foundation using higher-order shear deformation plate theories", *Smart Struct Syst*., **21**(1), 113-122. https://doi.org/10.12989/sss.2018.21.1.113.

Fourn, H., Ait Atmane, H., Bourada, M., Bousahla, A.A., Tounsi, A. and Mahmoud, S.R. (2018), "A novel four variable refined plate theory for wave propagation in functionally graded material plates", *Steel Compos. Struct.*, **27**(1), 109-122. https://doi.org/10.12989/scs.2018.27.1.109.

Hamidi, A., Houari, M.S.A., Mahmoud, S.R. and Tounsi, A. (2015), "A sinusoidal plate theory with 5-unknowns and stretching effect for thermomechanical bending of functionally graded sandwich plates", *Steel Compos. Struct*., **18**(1), 235-253. https://doi.org/10.12989/scs.2015.18.1.235.

Hanna, N.F. and Leissa, A.W. (1994), "A higher order shear deformationtheory for the vibration of thick plates", *J. Sound Vib*., **170**(4), 545-555. https://doi.org/10.1006/jsvi.1994.1083.

Hebali, H., Bakora, A., Tounsi, A. and Kaci, A. (2016), "A novel four variable refined plate theory for bending, buckling, and vibration of functionally graded plates", *Steel Compos. Struct*., **22**(3), 473-495. https://doi.org/10.12989/scs.2016.22.3.473.

Kar, V.R. and Panda, S.K. (2015a), "Large deformation bending analysis of functionally graded spherical shell using FEM", *Struct. Eng. Mech*., **53**(4), 661-679. https://doi.org/10.12989/sem.2015.53.4.661.

Karama, M., Afaq, K.S. and Mistou, S. (2003), "Mechanical behaviour of laminated composite beam by new multi-layered laminated composite structures model with transverse shear stress continuity", *Int. J. Solid. Struct*., **40**(6), 1525-1546. https://doi.org/10.1016/S0020-7683(02)00647-9.

Khetir, H., Bouiadjra, M.B., Houari, M.S.A., Tounsi, A. and Mahmoud, S.R. (2017), "A new nonlocal trigonometric shear deformation theory for thermal buckling analysis ofembedded nanosize FG plates", *Struct. Eng. Mech*., **64**(4), 391-402. https://doi.org/10.12989/sem.2017.64.4.391.

Kim, D.N. and Bathe, K.J. (2008), "A 4-node 3D-shell element to model shell surface tractions and incompressible behavior", *Comput. Struct.*, **86**, 2027-2041. https://doi.org/10.1016/j.compstruc.2008.04.019.

Kim, S.E., Thai, H.T. and Lee, J. (2009), "Buckling analysis of plates using the two variable refined plate theory", *Thin Wall. Struct.*, **47**(4), 455-462. https://doi.org/10.1016/j.tws.2008.08.002.

Lo, K.H., Christensen, R.M. and Wu, E.M. (1977), "A high-order theory of plate deformation. Part 2, Laminated plates", *J. Appl. Mech*., **44**(4), 669-676. https://doi.org/10.1115/1.3424155.

Mantari, J.L, Oktem, A.S. and Guedes Soares, C. (2012), "A new higher order shear deformation theory for sandwich and composite laminated plates", *Compos. Part B: Eng.*, **43**, 1489-1499. https://doi.org/10.1016/j.compositesb.2011.07.017.

Menasria, A., Bouhadra, A., Tounsi, A., Bousahla, A.A. and Mahmoud, S.R. (2017), "A new andsimple HSDT for thermal stability analysis of FG sandwich plates", *Steel Compos. Struct.*, **25**(2), 157-175. https://doi.org/10.12989/scs.2017.25.2.157.

Meziane, M.A.A., Abdelaziz, H.H. and Tounsi, A. (2014), "An efficient and simple refined theory for buckling and free vibration of exponentially graded sandwich plates under various boundary conditions", *J. Sandw. Struct. Mater*., **16**(3), 293-318. https://doi.org/10.1177/1099636214526852.

Mindlin, R.D. (1951), "Inuence of rotary inertia and shear on exural motions of isotropic, elastic plates", *J. Appl. Mech*., **18**, 31-38.

Nakasone, Y., Yoshimoto, S. and Stolarski, T.A. (2006), Engineering Analysis with Ansys Software, Elsevier, Butterworth-Heinemann Linacre House, Jordan Hill, Oxford OX2 8DP30 Corporate Drive, Burlington.

Narendar, S. (2011), "Buckling analysis of micro-/nano-scale plates based on two variable refined plate theory incorporating nonlocal scale effects", *Compos. Struct*., **93**(12), 3093-3103. https://doi.org/10.1016/j.compstruct.2011.06.028.

Noor, A.K. (1975), "Stability of multilayered composite plate", *Fibre. Sci. Technol*., **8**, 81-89. https://doi.org/10.1016/0015-0568(75)90005-6.

Pagano, N.J. (1970), "Exact solution for rectangular bidirectional composites and sandwich plates", *J. Compos.Mater*., **4**(1), 20-34. https://doi.org/10.1177/002199837000400102.

Patel, S.N. (2014), "Nonlinear bending analysis of laminated composite stiffened plates", *Steel Compos. Struct*., **17**(6), 867-890. http://dx.doi.org/10.12989/scs.2014.17.6.867.

Piscopo, V. (2010), "Refined buckling analysis of rectangular plates under uniaxial and biaxial compression", *World Acad. Sci., Eng. Technol*., **46**, 554-561.

Reddy, J.N. (1984), "A simple higher-order theory for laminated composite plates", *J. Appl. Mech*., **51**, 745-752. https://doi.org/10.1115/1.3167719.

Reddy, J.N. (1984), *Energy and Variational Methods in Applied Mechanics*, John Wiley and Sons, New York.

Reddy, J.N. (2004), *Mechanics of Laminated Composite Plates and Shells, Theory and Analysis*, 2nd Edition, CRC Press, New York.

Reddy, J.N. and Phan, N.D. (1985), "Stability and vibration of isotropic, orthotropic and laminated plates according to a higher-order shear deformation theory", *J. Sound Vib*., **98**(2), 157-170. https://doi.org/10.1016/0022-460X(85)90383-9.

Reissner, E. (1945), "The effect of transverse shear deformation on the bending of elastic plates", *J. Appl. Mech*., **12**, 69-77.

Reza Barati, M. and Shahverdi, H. (2016), "A four-variable plate theory for thermal vibration of embedded FG nanoplates under non-uniform temperature distributions with different boundary conditions", *Struct. Eng. Mech*., **60**(4), 707-727. https://doi.org/10.12989/sem.2016.60.4.707.

Rezaiee-Pajand, M. and Arabi, E. (2016), "A curved triangular element for nonlinear analysis of laminated shells", *Compos. Struct*., **153**(1), 538-548. https://doi.org/10.1016/j.compstruct.2016.06.052.

Rezaiee-Pajand, M., Arabi, E. and Masoodi, A.R. (2018), "A triangular shell element for geometrically nonlinear analysis", *Acta Mechanica*, **229**(1), 323-342. https://doi.org/10.1007/s00707-017-1971-8.

Rezaiee-Pajand, M., Masoodi, A.R. and Arabi, E. (2018), "Geometrically nonlinear analysis of FG doubly-curved and hyperbolical shells via laminated by new element", *Steel Compos. Struct.*, **28**(3), 389-401. http://dx.doi.org/10.12989/scs.2016.22.6.1445.

Rezaiee-Pajand, M., Masoodi, A.R. and Arabi, E. (2018), "On the shell thickness-stretching effects using seven-parameter triangular element", *Eur. J. Comput. Mech.*, **27**(2), 163-185. https://doi.org/10.1080/17797179.2018.1484208.

Rezaiee-Pajand, M., Shahabian, F. and Tavakoli, F.H. (2012), "A new higher-order triangular plate Bending element for the analysis of laminated composite and sandwich plates", *Struct. Eng. Mech*., **43**(2), 253-271. https://doi.org/10.12989/sem.2012.43.2.253.

Senthilnathan, N.R., Chow, S.T., Lee, K.H. and Lim, S.P. (1987), "Buckling of shear-deformable plates", *AIAA J*., **25**(9), 1268-1271. https://doi.org/10.2514/3.48742.

Shaheen, Y.B., Mahmoud, A.M. and Refat, H.M. (2016), "Structural performance of ribbed ferrocement plates reinforced with composite materials", *Struct. Eng. Mech*., **60**(4), 567-594. http://dx.doi.org/10.12989/sem.2016.60.4.567.

Shimpi, R.P. (2002), "Refined plate theory and its variants", *AIAA J.*, **40**(1), 137-46. https://doi.org/10.2514/2.1622.

Shimpi, R.P. and Patel, H.G. (2006), "A two variable refined plate theory for orthotropic plate analysis", *Int. J. Solid. Struct.*, **43**(23), 6783-6799. https://doi.org/10.1016/j.ijsolstr.2006.02.007.

Soldatos, K.P. (1992), "A transverse shear deformation theory for homogeneous monoclinic plates", *Acta Mech*., **94**(3), 195-200. https://doi.org/10.1007/BF01176650.

Soldatos, K.P. and Timarci, T. (1993), "A unified formulation of laminated composite, shear deformable, five-degrees-of-freedom cylindrical shell theories", *Compos. Struct.*, **25**(1-4), 165-171. https://doi.org/10.1016/0263-8223(93)90162-J.

Thai, H.T. (2012), "A nonlocal beam theory for bending, buckling, and vibration of nanobeams", *Int. J. Eng. Sci.*, **52**, 56-64. https://doi.org/10.1016/j.ijengsci.2011.11.011.

Thai, H.T. and Choi, D.H. (2012), "An efficient and simple refined theory for buckling analysis of functionally graded plates", *Appl. Math. Model.*, **36**(3), 1008-1022. https://doi.org/10.1016/j.apm.2011.07.062.

Thai, H.T. and Kim, S.E. (2010), "Free vibration of laminated composite plates using two variable refined plate theory", *Int. J. Mech. Sci.*, **52**, 626-633. https://doi.org/10.1016/j.ijmecsci.2010.01.002.

Touratier, M. (1991), "An efficient standard plate theory", *Eng. Sci.*, **29**(8), 901-916. https://doi.org/10.1016/0020-7225(91)90165-Y.

Whitney, J.M. and Sun, C.T. (1973), "A higher order theory for extensional motion of laminated composites", *J. Sound Vib.*, **30**(1), 85-97. https://doi.org/10.1016/S0022-460X(73)80052-5.

Xiang, S. and Kang, G.W. (2013b), "A nth-order shear deformation theory for the bending analysis on the functionally graded plates", *Eur. J. Mech. A/Solid.*, **37**, 336-343. https://doi.org/10.1016/j.euromechsol.2012.08.005.

Xiang, S., Jiang, S.X., Bi, Z.Y., Jin, Y.X. and Yang, M.S. (2011b), "A nth-order meshless generalization of Reddy's third-order shear deformation theory for the free vibration on laminated composite plates", *Compos. Struct.*, **93**(2), 299-307. https://doi.org/10.1016/j.compstruct.2010.09.015.

Xiang, S., Jin, Y.X., Bi, Z.Y., Jiang, S.X. and Yang, M.S. (2011a), "A n-order shear deformation theory for free vibration of functionally graded and composite sandwich plates", *Compos. Struct.*, **93**(11), 2826-2832. https://doi.org/10.1016/j.compstruct.2011.05.022.

Xiang, S., Kang, G.W. and Xing, B. (2012), "A nth-order shear deformation theory for the free vibration analysis on the isotropic plates", *Meccanica*, **47**(8), 1913-1921. https://doi.org/10.1007/s11012-012-9563-0.

Xiang, S., Kang, G.W., Yang, M.S. and Zhao, Y. (2013a), "Natural frequencies of sandwich plate with functionally graded face and homogeneous core", *Compos. Struct.*, **96**, 226-231. https://doi.org/10.1016/j.compstruct.2012.09.003.

Younsi, A., Tounsi, A., Zaoui, F.Z., Bousahla, A.A. and Mahmoud, S.R. (2018), "Novel quasi-3D and 2D shear deformation theories for bending and free vibration analysis of FGM plates", *Geomech. Eng.*, **14**(6), 519-532. https://doi.org/10.12989/gae.2018.14.6.519.

CC

Nomenclature

x, y, z	: coordinate reference system
u, v and w_0	: in-plane and transverse displacements of a point (x, y) on the mid-plane
u_1, u_2 and u_3	: displacements in x, y and z directions, respectively
ϕ_x and ϕ_y	: rotations of normal to the mid-plane
a	: length of the plate (meter)
b	: width of the plate (meter)
h	: Total thickness of the plate (meter)
a/h	: span-to-thickness ratio (Unit less)
E_1 and E_2	: Young's moduli along and transverse direction of the fiber (GPa)
G_{12}, G_{23}	: in-plane shear moduli (GPa)
G_{13}	: transverse shear moduli (GPa)
v_{12} and v_{21}	: Poison's ratios in respective plane (Unit less)
Q_{ij}	: plane stress reduced elastic constants in the material axes of the plate
$\overline{Q}_{ij}$	: transformed material constants
$A_{ij}, A_{ij}^s, D_{ij}, D_{ij}^s, H_{ij}^s$	: plate stiffness
θ	: fibre orientation angle
k	: total number of layers
U	: strain energy of the plate.
q	: transverse distributed loads
δ	: variation with respect to x and y respectively
$\sigma_x, \sigma_y, \sigma_{xy}, \sigma_{xz}, \sigma_{xz}$	: components of stress
$\varepsilon_x, \varepsilon_y, \gamma_{xy}, \gamma_{xz}^s, \gamma_{yz}^s$	: components of strain
$\overline{\sigma}_x, \overline{\sigma}_y, \overline{\sigma}_{xy}, \overline{\sigma}_{xz}, \overline{\sigma}_{yz}$	: non-dimensionlized stress components
$\overline{W}$	: non-dimensional transverse displacement
M_i^b, M_i^s, Q_j (i=x,y,xy, j=xz, yz)	: resultants moments, shear forces, respectively
m, n	: number of half waves in the x- and y-directions, respectively
w	: transverse displacement
w_b	: bending component of transverse displacement
W_s	: shear component of transverse displacement

T_1 and T_2 are the transformation matrix

CLPT	: classical laminate plate theory
FSDT	: first-order shear deformation theory
HSDT	: higher-order shear deformation theory
CU	: uniform distributed loads
CDS	: sinusoidal distributed loads